Excited states in 104Cd described with the interacting boson model plus broken pairs

De Angelis, G.; Fahlander, C.; Vretenar, Dario; Brant, Slobodan; Gadea, A.; Algora, A.; Li, Y.; Pan, Q.; Farnea, E.; Bonsignori, G.; ...

Journal article, Published version
Rad u časopisu, Objavljena verzija rada (izdavačev PDF)

Permanent link / Trajna poveznica: https://urn.nsk.hr/urn:nbn:hr:217:422505

Download date / Datum preuzimanja: **2024-04-19**

Repository / Repozitorij:

Repository of the Faculty of Science - University of Zagreb

Excited states in ^{104}Cd described with the interacting boson model plus broken pairs

G. de Angelis,[1] C. Fahlander,[1] D. Vretenar,[2] S. Brant,[2] A. Gadea,[1] A. Algora,[1,*] Y. Li,[1,†] Q. Pan,[1,‡] E. Farnea,[1] D. Bazzacco,[3] G. Bonsignori,[4] F. Brandolini,[3] M. De Poli,[1] D. De Acuna,[1] S. Lunardi,[3] G. Maron,[1] D. R. Napoli,[1] P. Pavan,[3] C. M. Petrache,[3] C. Rossi Alvarez,[3] P. Spolaore,[1] and G. Vedovato[1]

[1]*Istituto Nazionale di Fisica Nucleare, Laboratori Nazionali di Legnaro, I-35020 Legnaro, Italy*
[2]*Physics Department, Faculty of Science, University of Zagreb, Zagreb, Croatia*
[3]*Dipartimento di Fisica dell'Università and Istituto Nazionale di Fisica Nucleare, Sezione di Padova, I-35131 Padova, Italy*
[4]*Dipartimento di Fisica dell'Università and Istituto Nazionale di Fisica Nucleare, Sezione di Bologna, I-40126 Bologna, Italy*

The high-spin structure of ^{104}Cd has been studied through the ^{50}Cr(^{58}Ni,4p) reaction at a beam energy of 220 MeV. The level scheme has been extended up to an excitation energy of 11.9 MeV. Four collective structures have been identified based on two-quasineutron configurations. The low-lying states of both parities, as well as the main $\Delta I = 2$ regular structures observed at high spin, are described in the framework of the interacting boson-fermion model with broken pairs. [S0556-2813(99)02707-7]

I. INTRODUCTION

The light Cd isotopes, with $Z=48$ and $A \approx 104$ are, because of the effects of the $Z=50$ shell closure, almost spherical at low spins showing excited states in qualitative agreement with the prediction of a spherical quadrupole vibrational model [1]. At higher angular momentum weakly deformed structures can develop due to the deformation driving effects of the neutron intruder orbital $[550]1/2^-$ orbital from the $h_{11/2}$ subshell [2–4].

A simultaneous treatment of the vibrational and rotational degrees of freedom can be obtained in the framework of the interacting boson-fermion model (IBM/IBFM) [5], which provides a consistent description of the low-spin nuclear structure from the spherical SU(5) to the rotational SU(3) limit. The IBM/IBFM model is also particularly interesting because it is able to describe the physics of high-spin states [6] if, in addition to bosons, selective noncollective fermion pair states are included in the model space through the successive breaking of the correlated S and D pairs (s and d bosons). This extension of the model is especially relevant for transitional regions, where single-particle excitations and vibrational collectivity are dominant modes and no clear axis for cranking exists.

In the present paper we report on a detailed study of the low- and high-spin level structure of the $Z=48$, $N=56$ nucleus^{104}Cd performed with the γ-detector array GASP. In a recent study [7] the high spin states of the ^{104}Cd nucleus have been investigated. In this work we have confirmed the low spin states of ^{104}Cd identifying several new γ branches. The high spin part of the level scheme has been considerably extended. Among the various structures newly observed in

^{104}Cd, a decoupled band built upon the $\nu(h_{11/2})^2$ configuration has been identified. Calculations performed in the framework of the interacting boson-fermion model plus broken pairs reproduce in detail the structure of the states of both positive and negative parity up to high spin.

II. MEASUREMENTS AND RESULTS

The ^{104}Cd nucleus has been populated through the ^{58}Ni(^{50}Cr,4p) reaction at a beam energy of 220 MeV. The beam was delivered by the Tandem XTU accelerator of the Legnaro National Laboratories and γ rays have been detected using the GASP array [8] composed of 40 Compton-suppressed high-efficiency HPGe detectors and an inner BGO ball of 80 crystals. Events have been collected on tape when at least three Compton-suppressed Ge detectors and three BGO detectors fired in coincidence.

The target consisted of 2 self-supporting foils of isotopically enriched ^{58}Ni for a total thickness of 1.1 mg/cm^2. Typical beam intensities were around 3 pnA, giving a singles rate of ≈ 10 kHz in the individual Ge detectors and an event rate of ≈ 6 kHz. A total of 800 million triplefold and higher events have been collected. In order to select the reaction channel we have used, in addition to the GASP array, the Si-ball ISIS [9], which consists of 40 ΔE-E telescopes, each composed of two Si detectors of 130 and 1000 μm thicknesses, respectively. The Si array is mounted in the same geometry as the Ge detectors of the GASP array and covers ≈ 70% of the total solid angle. In the off-line analysis the 4p channel leading to ^{104}Cd was selected by requiring that only the events corresponding to the detection of four protons in the Si detectors were incremented into a symmetrized E_γ-E_γ matrix.

Energy calibration of the spectra and gain matching between the different Ge detectors have been performed using standard γ-ray sources as well as known γ-ray transitions of ^{104}Cd and of the neighboring nuclei populated in the same reaction. The data have been sorted into fully symmetrized matrices and cubes with proper conditions on the fold and on the sum energy of the BGO ball. In order to enhance the

---

*Permanent address: Institute of Nuclear Research of the Hungarian Academy of Sciences, Debrecen Pf. 51, H-4001, Hungary.

†Permanent address: Institute of Physics, Academia Sinica, Shanghai, P. R. China.

‡Permanent address: Institute of Modern Physics, Academia Sinica, Lanzhou, P.R. China.
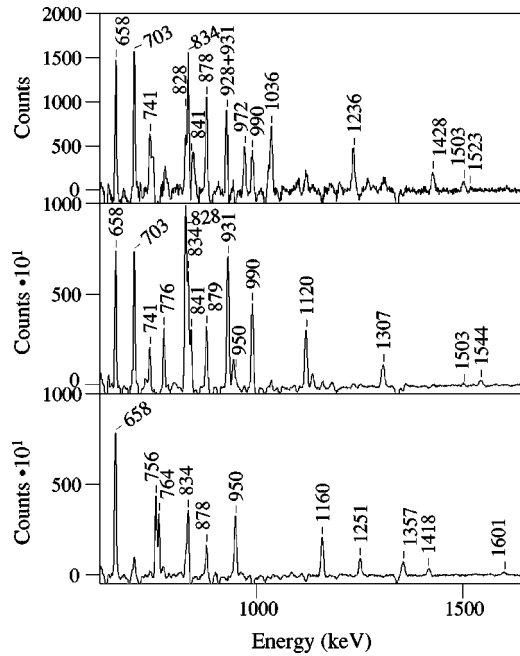
FIG. 1. Examples of sums of doubly gated spectra showing three of the high-spin structures in ^{104}Cd, namely, from the top, band 1, band 2, and band 3. The spectra are obtained gating on the combination of the 658, 834, 878 keV transitions with the 972, 1036, 1236, and 1428 keV lines (band 1), the 703, 990, 1120, and 1307 keV lines (band 2), and the 756, 764, 950, 1160, and 1251 keV lines (band 3). The energy labels are given in keV.

different band structures seen in ^{104}Cd we made use of the triples data by constructing γ-γ matrices in coincidence with the strongest transitions in each observed regular sequence. Such double gated coincidence events have been used for the main part of the data analysis. Examples of doubly gated spectra showing three of the high-spin structures in ^{104}Cd are given in Fig. 1.

The spins and parities of the levels have been deduced from the analysis of the directional correlation ratios from oriented states (DCO) for the ^{104}Cd transitions. A DCO γ-γ matrix has been created sorting on one axis the detectors placed at 90° with respect to the beam direction and on the other those at 34° and 146°. In the GASP geometry, if one gates on a stretched quadrupole transition, the theoretical DCO ratios $I_{34°}(\gamma)/I_{90°}(\gamma)$ are ≈ 1 for stretched quadrupole transitions and ≈ 0.5 for pure dipole transitions. If, on the contrary, gates are set on a pure dipole transition, the expected DCO ratios for quadrupole and dipole transitions are ≈ 2 and ≈ 1, respectively. The γ-ray energies and relative intensities of the γ-transitions belonging to ^{104}Cd, together with the DCO ratios and spin-parity assignments are reported in Table I.

III. THE LEVEL SCHEME OF ^{104}Cd

The level scheme of the ^{104}Cd nucleus deduced from the present study is shown in Fig. 2 and the information about the observed γ-ray transitions is summarized in Table I. The transitions have been placed in the level scheme on the basis

of coincidence relationships and relative intensities. Note that uncertainties of these values are subject to assumptions on shapes of the peaks and on the background subtraction procedure. The efficiency calibration uncertainty was estimated to be about 5%.

Spin assignments are based on the DCO analysis and on the decay patterns. The parity of the levels has been established assuming that, when gating on a $\Delta I = 2$ stretched quadrupole transition, the strong transitions with DCO ratios ≈ 1 have $E2$ character, the ones with DCO ratios ≈ 0.5 have $E1$ character and the transitions with DCO ratios definitely different from 1 and 0.5 are of mixed multipolarity ($M1 + E2$ character).

The excited high spin states of ^{104}Cd have been studied previously in Ref. [7]. We confirm all the known levels below the 12^+ state at 4820 keV of excitation energy. Several new decay branches connect the low lying states, resulting in a very complicated level structure and in a decay pattern typical of an almost spherical nucleus. Above 3.7 MeV of excitation energy the decay scheme changes, showing regular sequences of states extending up to $E_x \approx 11.9$ MeV — labeled from 1 to 4 in Fig. 2.

A complicated level structure has been observed above the $I^\pi = 12^+$ state at 4820 keV of excitation energy. Two transitions feeding the $I^\pi = 12^+$ level, the 909 and 973 keV γ lines, where also observed in Ref. [7] but placed in the level scheme in different positions.

A new cascade (band 1 in Fig. 2) consisting of 929, 972, 1036, 1235, and 1428 keV transitions of $E2$ character is observed and tentatively connected to the negative parity structure (band 2 in Fig. 2) through two γ transitions of 1503 and 1523 keV. The 1503 keV line, linking the cascade to the level at 6666 keV of excitation energy, is of dipole character suggesting a positive parity for this structure.

The negative parity band 2 was also observed in Ref. [7] up to 7.8 MeV of excitation energy but to the 931 keV transition was assigned a dipole character. In our data three transitions of 928.3, 929.4, and 931.3 keV are observed, the last one being by far the strongest. The DCO values for the 928.3 keV line (gating on the 1031.2 keV $10^+ \rightarrow 8^+$ transition) and for the sum of the other two γ lines (gating on the 841.2 keV $8^+ \rightarrow 6^+$ transition) suggest an $E2$ character for both the 928.3 keV $8^+ \rightarrow 6^+$ and the 931.3 keV $13^- \rightarrow 11^-$ transitions.

Three transitions of band 3 of 764, 756, and 950 keV, Fig. 2, were previously observed but placed in the level scheme in different order and position. Our ordering and placement is supported by the linking transitions to band 2 and to the low lying positive parity states.

Another sequence of transitions (band 4 in Fig. 2), consisting of the 672, 750, 778, and 1062 keV γ lines, has been observed, feeding the 10^+ level at 3656 keV of excitation energy and the 6^+ at 2371 keV. The 1357 keV line, linking the cascade to the 6^+ level at 2371 keV, is of dipole character suggesting a negative parity for this structure. The level scheme is completed with a few other single transitions feeding different levels.

TABLE I. Energies, relative intensities and DCO ratios of γ transitions assigned to ^{104}Cd from the ^{58}Ni$+^{50}$Cr reaction at 220 MeV.

E_γ (keV)	$I_\gamma{}^{a}$	DCO[b]	E_x (keV)	$J_i^\pi \to J_f^\pi$	E_γ (keV)	$I_\gamma{}^{a}$	DCO[b]	E_x (keV)	$J_i^\pi \to J_f^\pi$
79.4(4)	10(3)	0.99(20)	4820	$12^+ \to 11$	833.5(7)[d]	25(9)		5578	$12^- \to 11^-$
275.1(4)	9(3)	0.55(15)	4741	$11 \to 10$	834.4(3)[d]	923(130)	1.00(15)	1493	$4^+ \to 2^+$
308.1(3)	46(8)	0.95(15)	3212	$8^+ \to 8^+$	841.2(3)	268(40)	0.96(14)	3212	$8^+ \to 6^+$
312.5(6)	3(1)		4041	$9^- \to 7^-$	862.5(4)	27(5)	1.00(15)	3299	$8^+ \to 6^+$
321.8(3)	47(8)	0.99(15)	2437	$6^+ \to 4^+$	878.5(3)	586(70)	1.08(15)	2371	$6^+ \to 4^+$
341.5(3)	16(3)	0.54(7)	5162	$12^+ \to 12^+$	890.7(3)	237(38)	0.95(14)	4103	$10^+ \to 8^+$
366.6(3)	24(4)	0.49(7)	4156	$8^- \to 7^-$	908.5(3)	52(10)	0.50(10)	7155	$15 \to 14^+$
410.9(4)	14(2)	0.75(10)	4741	$11 \to 10^+$	928.3(3)	77(15)	0.94(18)	3299	$8^+ \to 6^+$
413.0(5)	8(3)	0.41(8)	4814	$10^- \to 9^-$	929.4(4)[e]			(7197)	$(14^+) \to (12^+)$
424.3(3)	18(4)	0.77(15)	4330	$10^+ \to 9^+$	931.3(3)[e]	210(35)	0.95(14)	5675	$13^- \to 11^-$
428.0(3)	70(13)	0.33(6)	4156	$8^- \to 7^-$	944.1(3)	198(30)	1.01(15)	2437	$6^+ \to 4^+$
448.8(4)	35(7)	0.55(8)	6246	$14^+ \to 13^+$	949.5(3)	82(17)	0.98(14)	7283	$16^- \to 14^-$
467.2(5)	14(3)	1.04(18)	2904	$8^+ \to 6^+$	965.0(5)	12(3)		5785	$\to 12^+$
500.4(4)	32(6)	1.19(15)	3033	$8^+ \to 6^+$	971.7(4)	22(8)	0.98(13)	(8169)	$(16^+) \to (14^+)$
532.7(4)	144(19)	1.02(14)	2904	$8^+ \to 6^+$	973.0(5)	15(6)	1.03(20)	8128	$17 \to 15$
546.8(5)	6(3)		8333	$\to 17^-$	976.6(4)	24(7)	0.69(8)	5798	$13^+ \to 12^+$
548.9(3)	14(3)	1.20(15)	6224	$15^- \to 13^-$	990.3(3)	118(19)	0.87(10)	6666	$15^- \to 13^-$
560.4(3)	27(5)	0.68(10)	4466	$10 \to 9^+$	997.0(6)	10(4)		(9125)	$\to 17$
616.0(5)	8(3)	0.4(1)	7283	$16^- \to 15^-$	1001.8(4)	55(9)	0.93(11)	3906	$10^+ \to 8^+$
622.4(2)	90(13)	0.75(10)	2115	$4^+ \to 4^+$	1031.2(5)	32(8)	1.00(15)	4330	$10^+ \to 8^+$
622.7(5)	23(4)	0.96(15)	3656	$10^+ \to 8^+$	1036.2(4)	34(8)	0.99(10)	(9205)	$(18^+) \to (16^+)$
635.3(4)	125(19)	0.91(10)	5455	$14^+ \to 12^+$	1040.2(4)	35(8)	0.98(11)	2533	$6^+ \to 4^+$
636.0(3)	31(6)	0.70(4)	5798	$13^+ \to 12^+$	1057.3(4)	29(6)	1.17(15)	5162	$12^+ \to 10^+$
640.6(4)	17(4)	0.58(9)	4744	$11^- \to 10^+$	1062.0(4)	20(6)		6991	$\to 13^-$
657.9(7)[c]			4814	$10^- \to 8^-$	1120.2(4)	70(13)	0.90(12)	7786	$17^- \to 15^-$
658.4(5)[c]			6334	$14^- \to 13^-$	1135.7(4)	27(7)	0.58(8)	4041	$9^- \to 8^-$
658.2(2)[c]	1000(100)	1.00(10)	658	$2^+ \to 0^+$	1158.1(7)	10(3)		4814	$10^- \to 10^+$
671.6(2)	17(4)	0.53(8)	6127	$\to 14^+$	1159.7(5)	57(10)	0.86(10)	8443	$18^- \to 16^-$
671.9(3)	59(10)	0.89(9)	4401	$9^- \to 7^-$	1184.7(5)	33(8)	0.84(8)	5929	$13^- \to 11^-$
703.4(3)	285(43)	0.94(10)	4744	$11^- \to 9^-$	1188.9(5)	11(2)	0.80(18)	4401	$9^- \to 8^+$
716.6(2)	137(21)	1.19(15)	4820	$12^+ \to 10^+$	1235.6(6)	13(5)	0.95(10)	(10440)	$(20^+) \to (18^+)$
741.3(3)	37(8)	0.45(7)	4041	$9^- \to 8^+$	1251.1(5)	27(7)	1.12(15)	9694	$20^- \to 18^-$
745.1(2)	22(4)	0.81(10)	4401	$9^- \to 10^+$	1307.3(6)	30(7)	1.12(16)	9093	$19^- \to 17^-$
749.6(2)	31(6)	0.97(13)	5151	$11^- \to 9^-$	1357.0(6)	75(14)	0.56(10)	3728	$7^- \to 6^+$
756.2(4)	95(15)	0.97(12)	6334	$14^- \to 12^-$	1418.2(8)	20(6)	0.56(10)	3787	$7^- \to 6^+$
763.5(4)	103(15)	0.93(13)	5578	$12^- \to 10^-$	1426.2(7)	27(5)	1.07(12)	4330	$10^+ \to 8^+$
768.0(4)	11(4)	0.92(10)	7013	$18^+ \to 16^+$	1427.7(8)	18(5)		(11868)	$\to (20^+)$
774.1(6)	16(5)	0.5(1)	4814	$10^- \to 9^-$	1503.0(7)	8(3)	0.4(2)	8169	$(16^+) \to 15^-$
775.8(3)	220(33)	0.91(14)	3212	$8^+ \to 6^+$	(1519(1))	4(2)		7197	$(14^+) \to 13^-$
778.1(4)	20(5)	1.00(20)	5929	$13^- \to 11^-$	(1523(1))	4(2)		6268	$(12^+) \to 11^-$
790.1(4)	25(5)	0.92(9)	6245	$16^+ \to 14^+$	1543.6(9)	7(3)	0.89(18)	10637	$21^- \to 19^-$
828.3(4)	229(34)	0.45(7)	4041	$9^- \to 8^+$	1600.6(9)	8(3)		11295	$\to 20^-$

[a]The relative intensities were normalized to the 658.2 keV $2^+ \to 0^+$ transition.

[b]DCO ratios are given for quadrupole gates.

[c]The relative intensity and the DCO ratio of the 658.2 keV transition includes also those of the unresolved 657.9 keV and 658.4 keV lines.

[d]The DCO ratio of the 834.4 keV transition includes also that of the unresolved 833.5 keV line.

[e]The relative intensity and the DCO ratio of the 931.3 keV transition includes also those of the unresolved 929.4 keV line.

IV. INTERACTING BOSON MODEL PLUS BROKEN PAIRS INTERPRETATION

The level scheme of ^{104}Cd, as deduced from the present work, displays a very complicated structure up to an excitation energy of about 3.7 MeV, whereas above that energy regular structures develop (labeled from 1 to 4 in Fig. 2). In the following we describe in detail the low-spin part of the level scheme in the framework of the interacting boson-fermion model. The extension of the model to include broken pairs allows also a description of high-spin states, and in particular calculations are performed for the bands labeled 2, 3, and 4. Of the other high-spin structures, the one built on

the 12^{+} state, band 1, can also be understood using the same formalism, even if a quantitative comparison between experiment and theory shows more discrepancies.

Models that are based on the interacting boson approximation (IBM) [10], provide a consistent description of the low-spin nuclear structure in spherical, deformed and transitional nuclei. By including part of the original shell-model fermion space through successive breaking of correlated S and D pairs, the IBM is extended to describe the structure of high-spin states. This extension of the model is especially relevant for transitional regions, where single-particle excitations and vibrational collectivity are dominant modes and no clear axis for cranking exists. The details of the model are
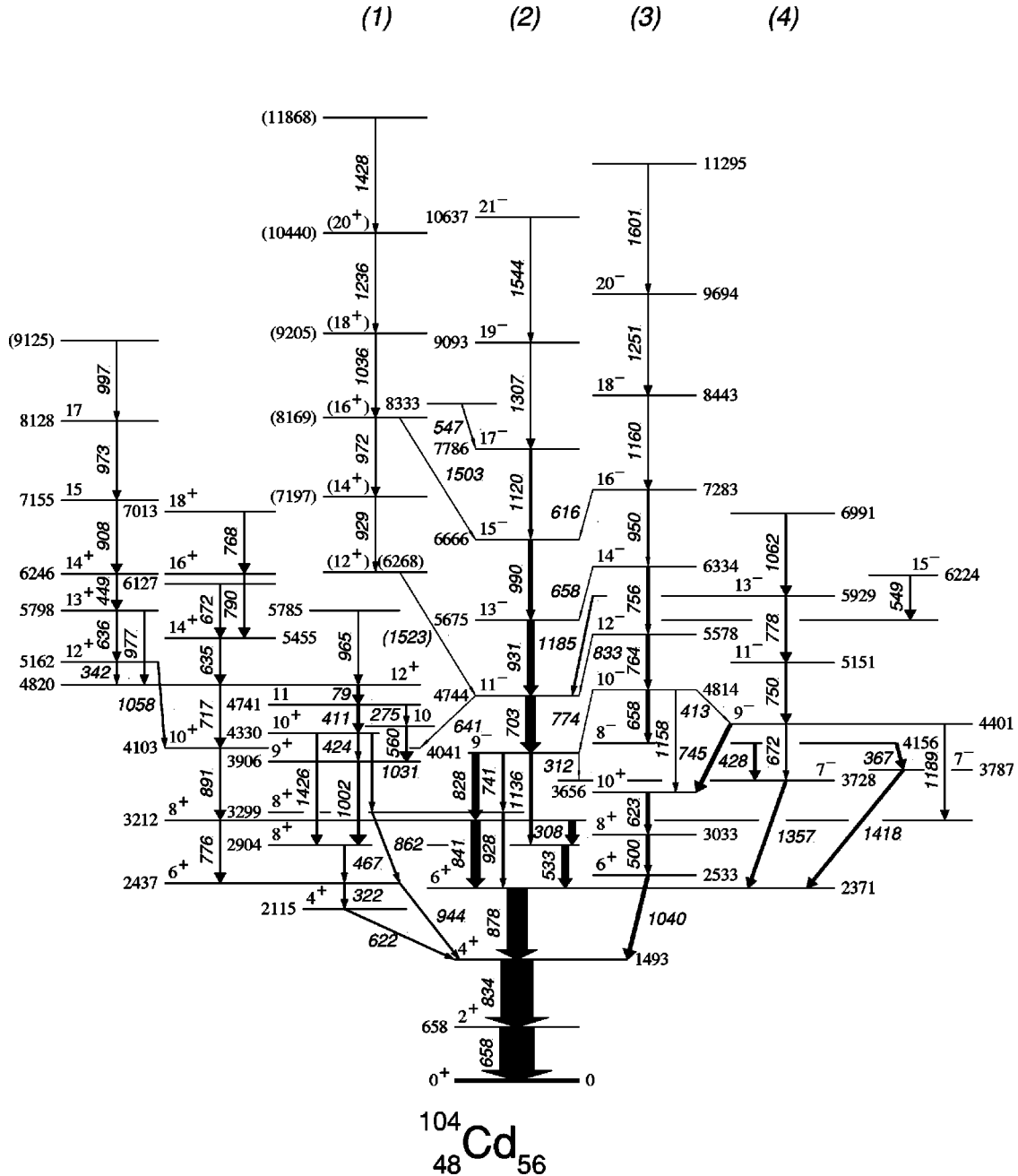

FIG. 2. Proposed level scheme of ^{104}Cd. The energy labels are given in keV. The widths of the arrows are proportional to the relative intensities.
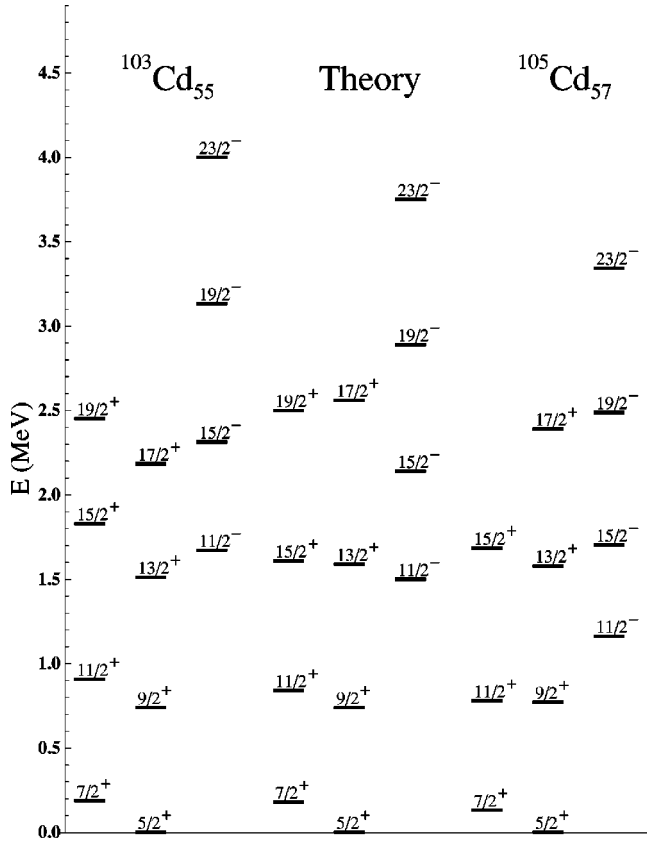
FIG. 3. Comparison between the experimental excitation energies of low-lying positive and negative parity states in ^{103}Cd and ^{105}Cd, and the levels calculated in the interacting boson-fermion model.

given in Refs. [6,11,12]. A short outline of the essential features follows.

The model is based on the IBM-1 [10]; the boson space consists of s and d bosons, with no distinction between protons and neutrons. To generate high-spin states, the model allows one or two bosons to be destroyed and noncollective fermion pairs to be formed, represented by two- and four-quasiparticle states which recouple to the boson core. High-spin states are described in terms of broken pairs. The model space for an even-even nucleus with $2N$ valence nucleons is

$$|N \text{ bosons}\rangle \oplus |(N-1) \text{ bosons} \otimes 1 \text{ broken pair}\rangle$$

$$\oplus |(N-2) \text{ bosons} \otimes 2 \text{ broken pairs}\rangle \oplus \cdots.$$

The model Hamiltonian has four terms: the IBM-1 boson Hamiltonian, the fermion Hamiltonian, the boson-fermion interaction, and a pair breaking interaction that mixes states with different number of fermions. In the present version of the model, we can only separately consider neutron or proton excitation and not mixed configurations. For odd-A nuclei [12], the IBFM plus broken pairs describes one- and three-fermion states. The model has been applied to the description of high-spin states in the Hg [6,11,12], Sr-Zr [13–15], and Nd-Sm [16–18] regions.

In general, most of the parameters of the Hamiltonian are taken from analyses of the low- and high-spin states in the neighboring even and odd nuclei. For ^{104}Cd the parameters of the boson Hamiltonian are $\epsilon = 0.658$ MeV, $C_4 = 0.117$ MeV, the number of bosons being $N = 4$. ϵ corresponds to the excitation energy of 2_1^+, and C_4 is adjusted to reproduce the 4_1^+ and 6_1^+ states. Since only the yrast sequence of the collective vibrational structure is known experimentally, the remaining parameters of the boson Hamiltonian could not be determined, and are set equal to zero. The resulting SU(5) vibrator spectrum displays very little anharmonicity. In the present calculation we only consider collective states and two-quasiparticle states based on configurations with two neutrons in the broken pair. States based on the proton $(g_{9/2})^2$ configuration, apart from the 0^+ and the 2^+ levels accounted by the boson Hamiltonian, are not included in the model space. The single-quasiparticle neutron energies and occupation probabilities are obtained by a simple BCS calculation using Reehal-Sorensen [19] single-particle energies. An additional shift of -0.1 MeV has been used for the $g_{7/2}$ single-particle energy. With a pairing strength $G = 23/A$, the resulting quasiparticle energies and occupation probabilities are $E(\nu d_{5/2}) = 1.113$ MeV, $E(\nu s_{1/2}) = 2.287$ MeV, $E(\nu h_{11/2}) = 2.691$ MeV, $E(\nu g_{7/2}) = 1.316$ MeV, $v^2(\nu d_{5/2}) = 0.57$, $v^2(\nu s_{1/2}) = 0.06$, $v^2(\nu h_{11/2}) = 0.04$, $v^2(\nu g_{7/2}) = 0.23$.

The parameters of the boson-fermion interactions have been adjusted to reproduce the lowest positive and negative parity structures in the neighboring odd-N isotopes ^{103}Cd and ^{105}Cd. For neutron states the boson-fermion parameters are $\Gamma_0 = 0.2$ MeV and $\chi = -0.9$ for the dynamical interaction, and $\Lambda_0 = 0.2$ MeV for the exchange interaction. In Fig. 3 we compare the lowest calculated decoupled structures based on the $d_{5/2}$, $g_{7/2}$, and $h_{11/2}$ neutron states, with the corresponding levels in ^{103}Cd and ^{105}Cd. Experimental data are from Refs. [20,21], and the theoretical spectrum is calculated with the IBFM-1 model [22]. As already mentioned the neutron model space contains the orbitals $\nu d_{5/2}$, $\nu s_{1/2}$, $\nu g_{7/2}$, and $\nu h_{11/2}$, and the number of bosons is $N = 4$. The calculated spectrum reproduces the trend of excited levels between ^{103}Cd and ^{105}Cd. The lowest two $\Delta I = 2$ bands are based on the $d_{5/2}$ and $g_{7/2}$ configurations, respectively. The calculation also reproduces the lowest negative parity band based on $h_{11/2}$. The corresponding boson-fermion interaction parameters have therefore been used in the calculation of two-neutron states in ^{104}Cd. In addition, the parameter of the boson quadrupole operator, $\chi = -0.9$, is adjusted to reproduce the experimental data for ^{106}Cd: $B(E2,2_1 \rightarrow 0_1) = 0.068 \ e^2 \ b^2$ and $Q(2_1) = -0.25 \ e$ b.

Results of model calculations for positive parity states in ^{104}Cd, with a fermion space of one neutron broken pair, are shown in Fig. 4. In addition to the boson and boson-fermion parameters that have already been discussed, here the strength parameter of the pair-breaking interaction is $U_2 = 0.1$ MeV. In this energy level diagram, only the few lowest calculated states of each spin are compared to the experimental counterparts. The collective vibrational structure remains yrast up to angular momentum $I = 6$. In the
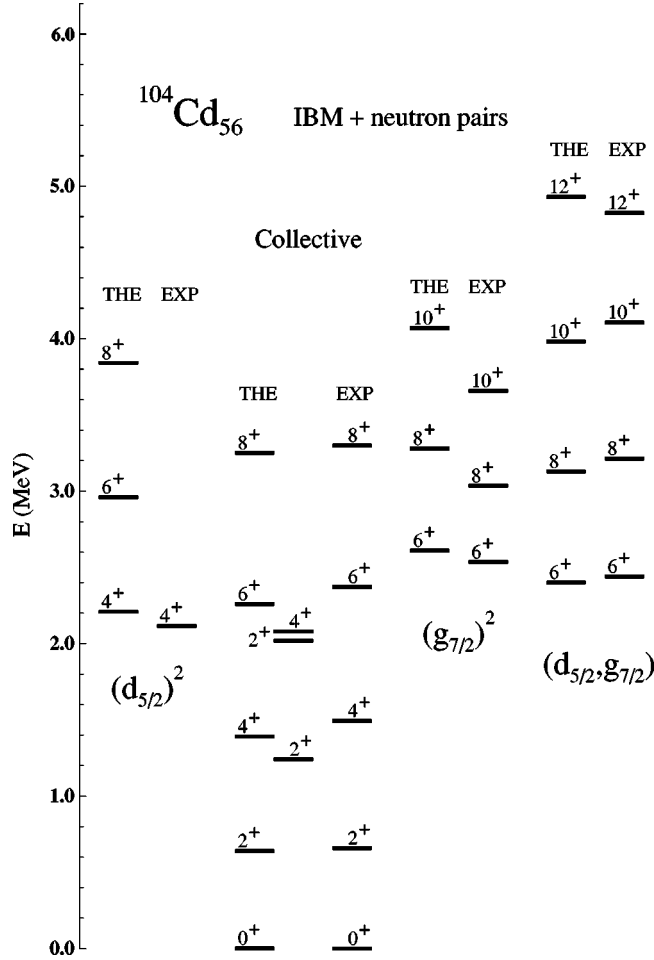
FIG. 4. Results of the IBM plus broken pair calculation for positive-parity states (THE) compared with experimental levels (EXP) in ^{104}Cd. The levels are grouped into bands according to the dominant components in the wave functions.

FIG. 5. Negative-parity states in ^{104}Cd (EXP) compared with results of the IBM plus broken pair calculation (THE). The levels are grouped into bands according to the dominant components in the model wave functions. Only states with possible experimental counterpart are shown.

experimental spectrum one finds four $I^\pi = 8^+$ states at 2904, 3033, 3212, and 3299 keV of excitation energy, respectively. In our calculations four $I^\pi = 8^+$ states are expected, the collective vibrational 8^+ state and three states based on the two neutron configurations $(d_{5/2})^2$, $(g_{7/2})^2$, and $(d_{5/2}, g_{7/2})$. For the two $\Delta I = 2$ positive parity sequences based on the $(g_{7/2})^2$ and $(d_{5/2}, g_{7/2})$ neutron configurations, probable experimental counterparts are observed (Fig. 4). The theoretical levels are grouped into bands according to the dominant components in the model wave functions. The state 8_1^+ at 2904 keV of excitation energy is known to be an isomer with $t_{1/2} \simeq 0.8$ ns [23], and is connected to the $6_{1,2}^+$ states by $B(E2)$ values of 0.5 and 0.7 Wu. It has probably a large $\pi(g_{9/2})_{8^+}^{-2}$ component as in ^{100,102}Cd [24,25], which is excluded from the model space. The two states with $I^\pi = 9^+$ and 10^+ observed at 3906 and 4330 keV, Fig. 2, decay to the 8_1^+ with 1002 and 1426 keV transitions, in general agreement with the excitation energy of 1206 keV of the 2^+ state in the ^{106}Sn core nucleus. The calculated energy spacings of the bands $(g_{7/2})^2$ and $(d_{5/2}, g_{7/2})$, Fig. 4, correspond to the collective vibrational sequence. The experimental energy spac-
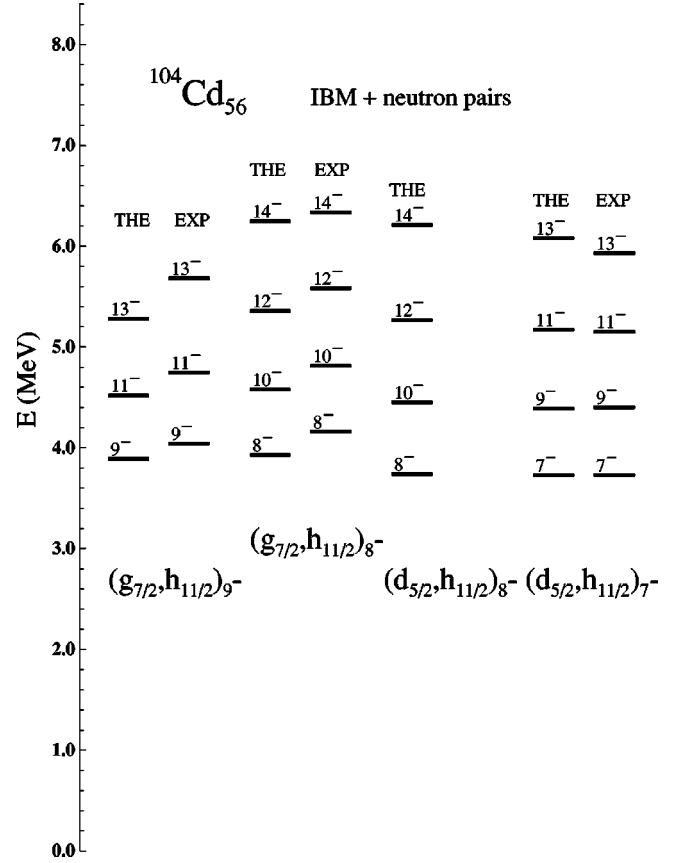
ings are somewhat smaller, indicating a stronger core polarization and/or change of deformation. This is probably caused by admixtures of $2p$-$2h$ proton configurations, an effect that could not be included in our model space.

In heavier Cd isotopes experimental data exist on the neutron $(h_{11/2})^2$ structure. The $I = 10^+$ bandhead of the $\Delta I = 2$ $(h_{11/2})^2$ sequence is at 4153 keV in ^{108}Cd [4] and 4816 keV in ^{106}Cd [3]. In ^{104}Cd this state is not observed. Our calculations place it at 5310 keV. The corresponding $I^\pi = 12^+$ and $I^\pi = 14^+$ of the band members based on the $(h_{11/2})_{10^+}^2$ state are calculated at 5940 and 6690 keV, respectively. We tentatively assign to this configuration the level structure built on the 12^+ state at 6268 keV of excitation energy. Compared to heavier isotopes, the ^{104}Cd nucleus has also less particles outside the closed shell and therefore collective properties are less pronounced. In particular, with only four bosons we can only construct states up to angular momentum $I = 16^+$, including the fermion space of two neutrons. States with higher angular momenta should be based on a different core including proton excitations across the $Z = 50$ shell closure.

The lowest calculated negative-parity two neutron states are compared with experimental levels in Fig. 5. The parameters of the Hamiltonian have the same values as in the cal-

culation of positive-parity states. Above 3.5 MeV of excitation energy several negative parity sequences with angular momenta ranging from $I = 7^-$ to $I = 9^-$ are observed in the experimental spectrum. In Fig. 5 the lowest two calculated $\Delta I = 2$ level sequences based on configurations with spin $I \geq 7^-$ are compared with experimental counterparts. The levels are grouped into sequences according to the dominant fermion component in the wave function. The two-fermion angular momentum is approximately a good quantum number. The collective part of the wave functions corresponds to that of the low-lying collective vibrational sequence. Because the quasiparticle energies of $d_{5/2}$ and $g_{7/2}$ differ by only ≈ 200 keV, both the $(h_{11/2}, d_{5/2})$ and the $(h_{11/2}, g_{7/2})$ configurations form sequences with states of the same angular momentum at almost the same excitation energies. The density of the expected negative parity states between 4 and 7 MeV is very high since all four neutron orbitals are included in the calculation, and one finds many states with low angular momenta which are not observed in the experimental data.

V. CONCLUSIONS

A rich level structure has been established in the vibrational nucleus ^{104}Cd by using the ^{58}Ni(^{50}Cr,4p) reaction. Four regular structures built on the $N = 5$ $\nu h_{11/2}$ intruder orbital have been identified and firmly connected to the lower-lying states. The main part of the level structure has been discussed in the framework of the interacting boson-fermion model extended by the inclusion of a broken pair. In particular, good agreement is found between calculations and experiment for the high-spin negative parity states based on $\nu(h_{11/2}), (d_{5/2}, g_{7/2})$ quasiparticle configurations as well as for low-lying states of positive parity.

ACKNOWLEDGMENTS

[1] M. Sambataro, Nucl. Phys. **A380**, 365 (1982).

[2] P.H. Regan, G.D. Dracoulis, G.J. Lane, P.M. Walker, S.S. Anderssen, A.P. Byrne, P.M. Davidson, T. Kibedy, A.E. Stuchbery, and K.C. Yeung, J. Phys. G **19**, L157 (1993).

[3] D. Jerrestam, F. Liden, J. Gizon, L. Hildingsson, W. Klamra, R. Wyss, D. Barneoud, J. Kownacki, Th. Lindblad, and J. Nyberg, Nucl. Phys. **A545**, 835 (1992).

[4] I. Thorslund, C. Fahlander, J. Nyberg, S. Juutinen, R. Julin, M. Piiparinen, R. Wyss, A. Lampinen, T. Lönnroth, D. Müller, S. Törmänen, and A. Virtanen, Nucl. Phys. **A564**, 285 (1994).

[5] F. Iachello and O. Scholten, Phys. Rev. Lett. **43**, 679 (1979).

[6] F. Iachello and D. Vretenar, Phys. Rev. C **43**, 945 (1991).

[7] W. Klamra, E. Adamides, A. Atac, R.A. Bark, B. Cederwall, C. Fahlander, B. Fogelberg, A. Gizon, J. Gizon, H. Grawe, E. Ideguchi, D. Jerrestam, A. Johnson, R. Julin, S. Juutinen, W. Kaczmarczyk, A. Kerec, J. Kownacki, S. Mitarai, L.O. Norlin, J. Nyberg, M. Piiparinen, R. Schubart, D. Seweryniak, G. Sletten, S. Törmänen, A. Virtanen, and R. Wyss, Z. Phys. A **352**, 117 (1995).

[8] D. Bazzacco, Report No. AECL 10613, 1992, Vol. 2, p. 376.

[9] E. Farnea, G. de Angelis, M. De Poli, D. De Acuna, A. Gadea, D.R. Napoli, P. Spolaore, A. Buscemi, R. Zanon, R. Isocrate, D. Bazzacco, C. Rossi Alvarez, P. Pavan, A.M. Bizzeti-Sona, and P.G. Bizzeti, Nucl. Instrum. Methods Phys. Res. A **400**, 87 (1997).

[10] F. Iachello and A. Arima, *The Interacting Boson Model* (Cambridge University Press, Cambridge, 1987).

[11] D. Vretenar, G. Bonsignori, and M. Savoia, Phys. Rev. C **47**, 2019 (1993).

[12] D. Vretenar, G. Bonsignori, and M. Savoia, Z. Phys. A **351**, 289 (1995).

[13] P. Chowdhury, C.J. Lister, D. Vretenar, Ch. Winter, V.P. Janzen, H.R. Andrews, D.J. Blumenthal, B. Crowell, T. Drake, P.J. Ennis, A. Galindo-Uribarri, D. Horn, J.K. Johansson, A. Omar, S. Pilotte, D. Prévost, D. Radford, J.C. Waddington, and D. Waed, Phys. Rev. Lett. **67**, 2950 (1991).

[14] C.J. Lister, P. Chowdhury, and D. Vretenar, Nucl. Phys. **A557**, 361c (1993).

[15] A.A. Chishti, P. Chowdhury, D.J. Blumenthal, P.J. Ennis, C.J. Lister, Ch. Winter, D. Vretenar, G. Bonsignori, and M. Savoia, Phys. Rev. C **48**, 2607 (1993).

[16] G. de Angelis, M.A. Cardona, M. De Poli, S. Lunardi, D. Bazzacco, F. Brandolini, D. Vretenar, G. Bonsignori, M. Savoia, R. Wyss, F. Terrasi, and V. Roca, Phys. Rev. C **49**, 2990 (1994).

[17] C. Rossi Alvarez, D. Vretenar, Zs. Podolyak, D. Bazzacco, G. Bonsignori, F. Brandolini, S. Brant, G. de Angelis, M. De Poli, M. Ionescu-Bujor, Y. Li, S. Lunardi, N.H. Medina, and C.M. Petrache, Phys. Rev. C **54**, 57 (1996).

[18] C.M. Petrache, R. Venturelli, D. Vretenar, D. Bazzacco, G. Bonsignori, S. Brant, S. Lunardi, N.H. Medina, M.A. Rizzutto, C. Rossi Alvarez, G. de Angelis, M. De Poli, and D.R. Napoli, Nucl. Phys. **A617**, 228 (1997).

[19] B.S. Reehal and R.A. Sorensen, Phys. Rev. C **2**, 819 (1970).

[20] M. Palacz, J. Cederkäll, M. Lipoglavsek, J. Person, A. Atac, J. Blomqvist, H. Grawe, C. Fahlander, A. Johnson, A. Kerek, J. Kownacki, A. Likar, L.-O. Norlin, J. Nyberg, R. Schubart, D. Seweryniak, Z. Sujkowski, R. Wyss, G. de Angelis, P. Bednarczyk, Zs. Dombradi, D. Foltescu, D. Jerrestam, S. Juutinen, E. Mäkelä, G. Perez, M. De Poli, H.A. Roth, T. Shizuma, Ö. Skeppstedt, G. Sletten, S. Törmänen, and T. Vass, Nucl. Phys. **A624**, 210 (1997).

[21] J. Genevey-Rivier, J. Treherne, J. Daniere, R. Berand, M. Mayer, and R. Rougny, J. Phys. G **4**, 943 (1978).

[22] F. Iachello and O. Scholten, Phys. Rev. Lett. **43**, 679 (1979); F. Iachello and P. Van Isacker, *The Interacting Boson-Fermion*

Model (Cambridge University Press, Cambridge, 1991).
[23] J. Blachot, Nucl. Data Sheets **64**, 1 (1991).
[24] M. Górska, R. Schubart, H. Grawe, J.B. Fitzgerald, D.B. Fossan, J. Heese, K.H. Maier, M. Rejmund, K. Spohr, and T. Rzaca-Urban, Z. Phys. A **350**, 181 (1995).
[25] J. Persson, J. Cederkäll, M. Lipoglavšek, M. Palacz, A. Ataç,

J. Blomqvist, C. Fahlander, H. Grawe, A. Johnson, A. Kerek, W. Klamra, J. Kownacki, A. Likar, L.-O. Norlin, J. Nyberg, R. Schubart, D. Seweryniak, G. de Angelis, P. Bednarczyk, Zs. Dombradi, D. Foltescu, S. Juutinen, E. Mäkelä, G. Perez, M. de Poli, H.A. Roth, T. Shizuma, Ö. Skeppstedt, G. Sletten, S. Törmänen, and T. Vass, Nucl. Phys. **A627**, 101 (1997).